

We solve the quadratic equation for α for different values of the ratio $R(\Sigma\pi/\Lambda\pi)$. The two solutions are plotted as a function of $R(\Sigma\pi/\Lambda\pi)$ in Fig. 9(a). The solutions are (i) $0 \leq \alpha \leq 0.18$ and (ii) $-0.31 \leq \alpha \leq 0$. [Note that the experimental value of $R(\Sigma\pi/\Lambda\pi) = 0.1 \pm 0.1$.] For each of the allowed values of α we calculate the predicted value of $\sigma(\bar{K}N)$ and compare it with the experimental result $3 < \sigma(\bar{K}N) < 7.6$. This is shown graphically in Fig. 9(b). Only the solution where α is negative is allowed and α must be within the limits $-0.31 < \alpha < -0.1$. This result is consistent with prediction based on the analysis of Kernan and Smart²¹

²¹ Anne Kernan and W. M. Smart, Lawrence Radiation Laboratory Report No. UCRL-17009 (unpublished); Phys. Rev. Letters **17**, 832 (1966).

of the relative phases of resonant amplitudes in the reaction $K^-n \rightarrow \Lambda\pi^-$ from 1650 to 1900 MeV.

ACKNOWLEDGMENTS

We would like to thank the Brookhaven National Laboratory 30-in. bubble chamber group and the AGS staff who made this experiment possible. The assistance of Dr. A. J. Herz, Dr. A. M. Aitken, and Dr. M. C. Whatley in various phases of the experiment are gratefully acknowledged. We would like to thank Dr. W. Willis, Dr. R. Ely, Dr. R. W. Birge, Dr. R. Levi-Setti, and Dr. M. Ferro-Luzzi for allowing us to use some of their data in this analysis and Dr. S. Meshkov for illuminating discussions. We would like to acknowledge the help of the Physics Department, University of Arizona, in completing the manuscript.

Polarization and Angular Distributions of Σ^0 from $\pi^- p \rightarrow K^0 \Sigma^0$ near 1.3 BeV/c*

R. L. CROLIUS,[†] V. COOK,[‡] BRUCE CORK, D. KEEFE, L. T. KERTH,
W. M. LAYSON,[§] AND W. A. WENZEL

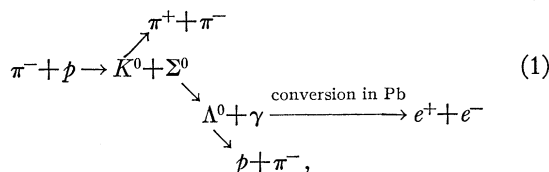
Lawrence Radiation Laboratory, University of California, Berkeley, California

(Received 27 May 1966; revised manuscript received 14 November 1966)

Production of $\Sigma^0 + K^0$ by π^- 's incident on liquid hydrogen has been studied in the π^- momentum region from 1200 to 1400 MeV/c. By means of spark chambers, the Σ^0 production angular distribution and polarization have been measured at four incident π^- momenta. Significant polarization, $\alpha_{\Lambda} P_{\Sigma} = -0.71_{-0.25}^{+0.38}$, exists in the backward hemisphere of Σ^0 production in the π^- momentum region from 1300 to 1350 MeV/c.

I. INTRODUCTION

WE detected associated production of Σ^0 's by π^- mesons incident on liquid hydrogen, recording the spark-chamber events photographically. Charged secondaries arising from the production and decay sequences



were detected in semicylindrical spark chambers. Topologically the events appear as two vees plus a γ -ray conversion pair. The primary goal of the experi-

ment was to look for a region of large Σ^0 polarization, because with polarized Σ^0 's the $\Sigma\Lambda$ relative parity can be measured by a method¹⁻³ independent of those used heretofore.⁴⁻⁶ The polarization of the decay lambdas from $\Sigma^0 \rightarrow \Lambda^0 + \text{Dalitz pair}$, is correlated with the orientation of the plane of the Dalitz pair in a way that depends on the Σ^0 relative parity. Measurement of the Σ^0 parity using this technique does not depend in any essential way upon other results, as do other methods that have been used.⁴⁻⁶

II. EXPERIMENTAL APPARATUS

The incident π^- beam, with momentum in the range 1200 to 1400 MeV/c, was produced from an internal target at the Bevatron. A conventional beam-transport

* This work was done under the auspices of the U. S. Atomic Energy Commission.

[†] Present address: Aerospace Corporation, San Bernardino, California.

[‡] Present address: University of Washington, Seattle, Washington.

[§] Present address: Pan American World Airways, Patrick Air Force Base, Florida.

¹ J. Sucher and G. A. Snow, Nuovo Cimento **18**, 195 (1960).

² N. Byers and H. Burkhardt, Phys. Rev. **121**, 281 (1961).

³ B. N. Valuev and B. V. Geshenbein, Zh. Eksperim. i Teor. Fiz. **39**, 1046 (1960) [English transl.: Soviet Phys.—JETP **12**, 728 (1961)].

⁴ R. H. Dalitz and B. W. Downs, Phys. Rev. **111**, 967 (1958).

⁵ J. Leitner, L. Gray, E. Harth, S. Lichtman, and J. Westgard, Phys. Rev. Letters **7**, 264 (1961).

⁶ H. Courant *et al.*, Phys. Rev. Letters **10**, 409 (1963); C. Alff, N. Gelfand, V. Nauenberg, M. Nussbaum, J. Schultz, and J. Steinberger, Phys. Rev. **137**, B1105 (1965).

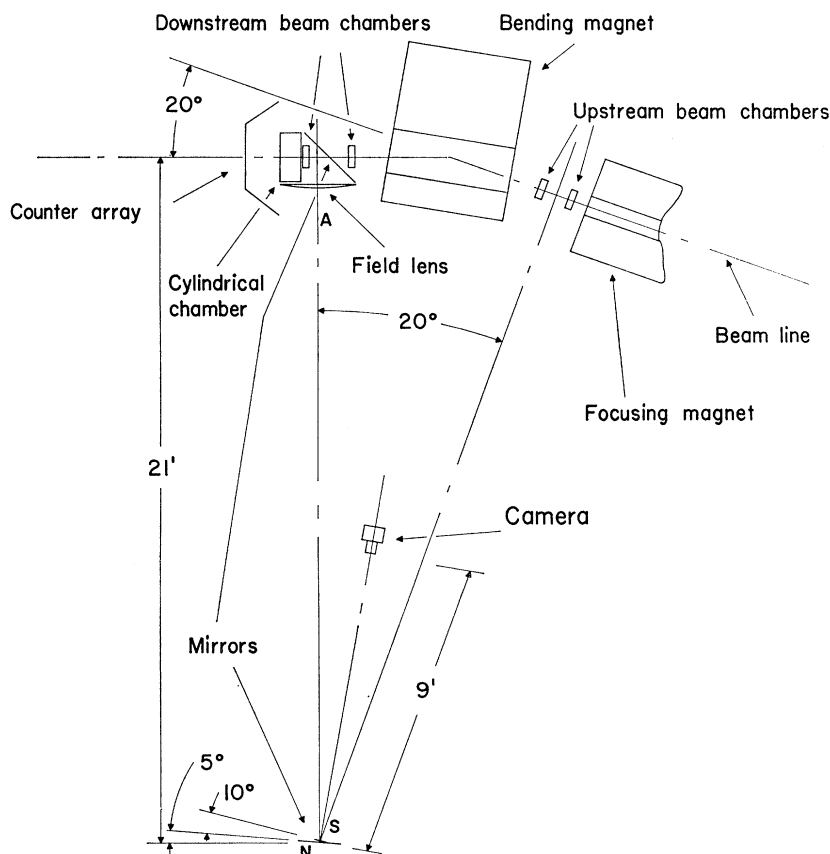


FIG. 1. Plan view of apparatus and optical arrangement.

system was used to convey the π^- from the production target to a liquid-hydrogen secondary target. The hydrogen target was a 3-in.-diam, 6-in.-long cylinder with its axis perpendicular to the beam direction. The target and detection apparatus were placed at the downstream end of a bending magnet (see Fig. 1), which dispersed the beam so that images of the internal target for various momenta were spread along the axis of the liquid-hydrogen target. The momentum of each beam particle could be determined by measuring tracks in beam-defining spark chambers placed at the entrance and exit of the bending magnet.

The detectors for the secondaries were two coaxial semicylindrical spark chambers viewed axially. Stereo information was provided by photographing spark images obtained by reflection of light circumferentially around the gaps⁷ (see Fig. 2). The plates were 0.003-in.-thick, hand-polished aluminum foil. A $\frac{1}{16}$ -in.-thick lead plate between the inner four-gap and outer six-gap chambers effected the conversion of γ rays from the $\Sigma^0 \rightarrow \Lambda^0 + \gamma$ decays. Spark resolution was 0.75 mm for tracks normal to the spark-chamber plates.

From Fig. 2 it can be seen that a bona fide event is expected to lead to six charged particles in the final

state, with two of them (electron pair) very close together. The triggering logic therefore demanded simultaneously (a) an incident pion, identified by scintillation and Cerenkov counters in the beam, and (b) five or more time-coincident particles emerging from the hydrogen target. This latter requirement was accomplished by surrounding the spark chambers with an array of 48 continuous scintillation counters whose signals provided the inputs to an adder discriminator.

Figure 2 shows the experimental apparatus. Views of the various chambers have been taken from a photograph of an actual event and superimposed on the drawing. Sparks appeared to be twice as intense in the direct view of the semicylindrical chambers as in the stereo view. Hence, neutral-density filters were used to equalize apparent spark intensities.

The system was designed to minimize systematic errors in several ways: The liquid-hydrogen target, spark chambers, and detecting counters had both up-down and left-right symmetry. The spark-chamber electrode supports and the fiducial boxes were accurately machined, and machined fiducial markings permitted optical alignment of the mirrors and spark chambers with the camera boresight. Imperfections in the chambers could cause local but not systematic spark position errors. (Spark broadening from small imperfec-

⁷ This method of stereo photography was suggested by A. Buffington.

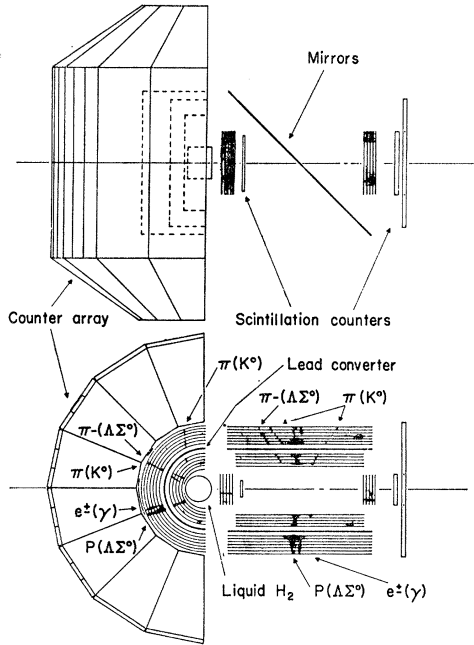


FIG. 2. Schematic diagram of counters and spark chambers, with a photograph of an event superimposed.

tions was observed.) Symmetry between the two possible images of some sparks in the stereo view provided a good test for systematic errors. None were observed. Large-scale optical distortions (e.g., those distortions caused by the field lenses) were corrected using the accurately located fiducials recorded on each frame.

III. DATA REDUCTION AND ANALYSIS

From 1.2 million photographs, 304 unambiguous $\Sigma^0 K^0$ events were obtained. The Λ^0 and K^0 decay vertices were not usually in the visible region of the chambers, so it was most practical to measure every event with four charged secondaries and an apparent conversion pair, unless the four tracks formed a star or a kinematically impossible configuration. Hence an event was measured if it had four tracks kinematically consistent with production of a neutral pair at a point in the hydrogen target, plus gamma conversion electrons emerging from a point in the lead. The only events excepted were stars; the scanner rejected these if extensions of all four secondary tracks and the beam pion track passed through a $\frac{1}{8}$ -in.-diam circle. This procedure prevented loss of events from judgment errors in scanning.

The SCAMP digitized measuring projectors with magnetic-tape storage were used for the film measurements.

It should be noted that in this cylindrical geometry the straight particle tracks do not in general appear straight in the stereo view, where the sparks are seen after tangential reflections. The track images are

sections of hyperbolas. Most tracks, however, appeared nearly straight, and were reconstructed by using the tangents at both ends of each track image.

There was sufficient information to do an over-all 1C fit. However, to minimize programming problems a simplified procedure, adequate to eliminate background, was adopted. Each measured event was checked for consistency and for rough kinematical fit. The approximately 710 events surviving these preliminary checks were subjected to a χ^2 test. The chosen χ^2 function was based on a simple fitting procedure which iteratively adjusted the angles of the four tracks from the Λ^0 and K^0 decays. Because the momentum and position of the incident pion were accurately measured and because the kinematical fit is insensitive to the γ -ray parameters, these tracks were not adjusted in the fitting procedure. The χ^2 function used was

$$\sum_{i=1,4} \left[\left(\frac{\theta_i - \theta_i^0}{\sigma_i(\theta_i)} \right)^2 + \left(\frac{\Phi_i - \Phi_i^0}{\rho_i(\Phi_i)} \right)^2 \right], \quad (2)$$

where Φ_i^0 and θ_i^0 are, respectively, the measured azimuth and dip angles of the i th track, ($1 \leq i \leq 4$), Φ_i and θ_i are the adjusted angles, and the angular uncertainties ρ_i and σ_i were estimated as functions of plate-to-track angles in dip and azimuth from measured values of spark scatter and width; other errors were assumed to be negligible by comparison. For example, σ_i varies from 2.2° in dip angle at zero dip angle to 4.8° at a 45° dip angle; and ρ_i is 2.2° in azimuth for a radial track and 3.3° for a track at 45° to a radius. These examples apply to tracks seen only in the inner four-gap chamber; errors were smaller for tracks seen in both chambers.

The distribution in χ^2 obtained for all events was as expected except that it included an excess of events with relatively large values for χ^2 . Efforts to associate χ^2 dependence with particular track geometry or other variables were unsuccessful, with one exception. It was found that large χ^2 was often correlated with events in which the scattering angle in the lead predicted for at least one secondary was larger than the assumed measuring error. When events with a predicted scattering angle (based on a fit or near fit) larger than the measurement error were remeasured using the inner (unscattered) portion of the track only, the χ^2 distribution improved somewhat.

Approximately 1/7 of the measured events were acceptable for the Σ^0 polarization analysis. Of the events that failed to pass as $\Sigma^0 K^0$, approximately half were judged to have gross qualitative defects that made questionable their original selection by scanners. The rest were attributed mainly to stars with single secondary scatterings and to events with multiple-beam tracks.

To avoid various scanning and triggering biases for the differential cross-section analysis, a geometrical cutoff was imposed. About $\frac{3}{5}$ of the sample for the

polarization measurement survived the cutoff and were used for the differential cross-section analysis. The detection efficiency of the system, which was particularly low for forward Σ^0 production, was evaluated with a Monte Carlo computer program as a function of hyperon center-of-mass (c.m.) production angle and pion-beam momentum; the results were used to correct the observed angular distributions to obtain the angular distributions presented here.

In the method used, a $\Sigma^0 K^0$ event for a particular Σ^0 production angle was generated, based on random number selection of the Σ^0 production point in the target, $\Sigma^0 K^0$ production plane orientation, and Λ^0 and K^0 path lengths, decay azimuths, and polar angles. With all the tracks thus determined in space, the geometry of the chambers and counters determined whether the event would have been detected. The Monte-Carlo-generated events that satisfied the detection geometry were analyzed by the fitting program to determine χ^2 values for every possible assignment of track labels. Ambiguities are possible in the Σ^0 and Λ^0 decay angles, as well as in particle identification, particularly because there is no indication of the charge or momentum of individual particles. Unambiguous cases only (i.e., unambiguous within our resolution) were included in the final samples of both Monte Carlo and real events. The only oversimplifications made in this analysis are (a) errors in track measurement were neglected in the Monte Carlo events before analysis by the fitting program, and (b) in the analysis of the angular distributions the Σ^0 's were assumed to be unpolarized. This latter assumption could not alter significantly the angular distributions because of the symmetry of the experimental apparatus and the insensitivity of our detection efficiency to the Σ^0 polarization.

Background was studied with the Monte Carlo program for various types of events that could simulate $\Sigma^0 K^0$. Events generated in this way were tested for $\Sigma^0 K^0$ fit. In this manner the probability that $\Lambda^0 K^0 \pi^0$ could simulate $\Sigma^0 K^0$ was found to be $\sim 20\%$. Hence $\Lambda^0 K^0 \pi^0$ background was judged not to be troublesome because (a) the Λ^0 's are not likely to be polarized in a

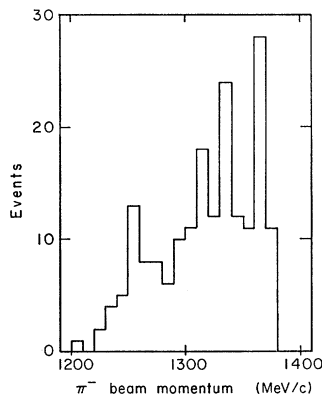


FIG. 3. Momentum histogram of incident π^- for events used in the angular-distribution analysis and total-cross-section calculation.

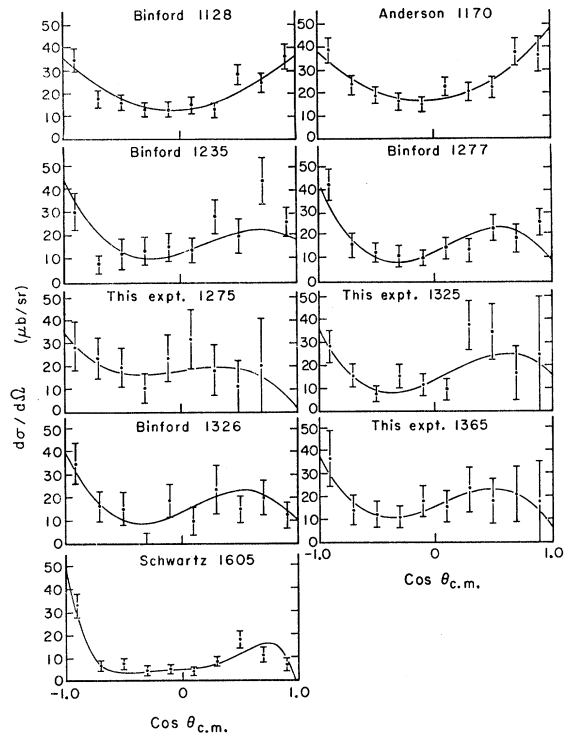


FIG. 4. Differential cross section for $\pi^- + p \rightarrow \Sigma^0 + K^0$. The solid curves represent cosine power-series fits from Table I.

way that would distort the apparent Σ^0 polarization, and (b) the $\Lambda^0 K^0 \pi^0$ cross section is low (~ 0.01 mb at these energies). We estimate that there was less than 1% $\Lambda^0 K^0 \pi^0$ contamination.

Production of $\Lambda^0 K^0$ plus an accidental γ ray could simulate $\Sigma^0 K^0$. Such background would be particularly troublesome because the Λ^0 polarization could distort the apparent Σ^0 polarization. The measurement of single-beam tracks at high intensity showed less than 1% of these events with tracks resembling γ -ray conversions. The Monte Carlo analysis shows that the probability that $\Lambda^0 K^0 \gamma$ simulated $\Sigma^0 K^0$ is 15%; hence contamination from such events should be $\lesssim 0.15\%$.

Contamination by $p\pi^-\pi^+\pi^-\pi^0$ and $p\pi^-\pi^+\pi^-\gamma$ were estimated to be insignificant because of the small production cross sections involved.

The selected events were tested for anomalies that would indicate biases or scanning inconsistencies. The spatial distribution of all measured particle tracks was inspected for irregularities and was compared with a Monte Carlo calculation of the expected distribution. The intersections of all measured tracks with the counter array were calculated; analysis showed that there were no biases from counter inefficiencies. The Λ^0 angular distribution in the Σ^0 c.m. system was found to be isotropic as expected. The observed pion angular distribution in the K^0 c.m. system for the experimental sample agreed well with that predicted from the corresponding Monte Carlo sample. The distribution of

TABLE I. Coefficients of cosine power-series fits for $\pi^- + p \rightarrow \Sigma^0 + K^0$.

Momen- tum (MeV/c) refer- ence	1129 Binford ^a	1170 Anderson ^b	1235 Binford ^a	1277 Binford ^a	1275 This expt.	1325 This expt.	1326 Binford ^a	1365 This expt.	1605 Schwartz ^c
A_0	13.2±1.4	12.8±1.5	14.2±2.2	13.3±1.8	17.7±5.7	13.4±3.0	12.6±2.2	15.5±3.6	4.4±1.2
A_1	0.72±2.0	3.8±2.2	17.7±6.1	24.1±5.8	8.1±15.9	23.3±9.7	19.0±7.3	19.9±11.8	0.7±6.3
A_2	22.8 ±4.1	20.8±4.3	20.4±6.6	14.8±4.8	1.4±23.9	13.4±11.6	12.1±5.9	7.0±11.8	12 ±11
A_3			-32.2±9.5	-42.2±9.5	-24.2±37.1	-33.5±19.2	-34.8±12.0	-36.8±22.8	49 ±29
A_4									6 ±15
A_5									-77 ±29
No. of events	738	322	257	315	44	78	168	50	117
Normal- ization (μb)	262 ±15	248	264 ±25	229 ±20	228 ^d	225 ^d	209 ±25	225 ^d	121

^a Reference 10.

^b Reference 11.

^c Reference 12.

^d Not a measured cross section.

the beam-interaction points in the target was also as expected. Aside from a failure of the scanners to detect large scatterings in the lead, as noted above, the only scanning bias found was against events with a decay in the spark chambers. This bias was found and corrected by eliminating the events that decay in the chambers from both Monte Carlo and real events.

The polarization analysis used a maximum-likelihood function based on Λ^0 decay as an analyzer. In particular, the Λ polarization is

$$\mathbf{P}_\Lambda = -(\mathbf{P}_\Sigma \cdot \hat{k})\hat{k}, \quad (3)$$

where \mathbf{P}_Σ is the Σ^0 polarization and \hat{k} is the direction of the decay γ ray in the Σ^0 c.m. system. The Λ^0 -decay angular distribution is given by

$$I(\theta) = \frac{1}{2}(1 + \alpha_\Lambda P_\Lambda \cos\theta), \quad (4)$$

where θ is the angle in the Λ^0 c.m. system between the direction of Λ^0 polarization and the momentum of the decay pion; the experimental value^{8,9} of α_Λ is -0.62 ± 0.05 .

The likelihood function used was

$$\mathcal{L}(\alpha_\Lambda P_\Sigma) = \prod_i [1 - \alpha_\Lambda P_\Sigma (\hat{N}_i \cdot \hat{k}_i)_\Sigma (\hat{k}_i \cdot \hat{k}_\pi)_\Lambda], \quad (5)$$

where i denotes the i th event, \hat{k}_i is the γ -ray momentum from Eq. (3), \hat{N}_i is the direction of \mathbf{P}_Σ , \hat{k}_π is the momentum of the decay pion, and the outer subscripts refer to the appropriate rest system for computing each kinematic factor. Errors associated with values of $\alpha_\Lambda P_\Sigma$ found in this way were taken to be the half-widths of the likelihood functions at $e^{-1/2}$ of the maximum heights.

⁸ E. F. Beall, Bruce Cork, D. Keefe, P. G. Murphy, and W. A. Wenzel, Phys. Rev. Letters **7**, 285 (1961).

⁹ J. W. Cronin and O. E. Overseth, Phys. Rev. **129**, 1795 (1963).

IV. RESULTS

A. Total Cross Section

The distribution in pion-beam momentum of all events is shown in Fig. 3. The average production cross section for these events is $220 \pm 20 \mu\text{b}$, in excellent agreement with Binford's values of 264 ± 25 , 229 ± 20 , and $209 \pm 25 \mu\text{b}$ at $p_\pi = 1235$, 1277 , and $1326 \text{ MeV}/c$, respectively.¹⁰ For our data it was impossible to measure the energy dependence of the production cross section, because the momentum distribution of our incident beam was not well known.

B. Angular Distribution

Our angular distributions, along with those of other experimenters,¹⁰⁻¹² are shown in Fig. 4. The smooth

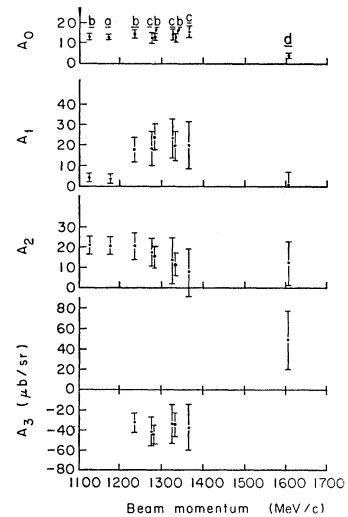


FIG. 5. Coefficients A_n , from Table I, of cosine power-series $d\sigma/d\Omega = \sum_n A_n \cos^n\theta$ as a function of beam momentum; (a) denotes Anderson, (b) Binford, (c) this experiment, and (d) Schwartz.

¹⁰ Thomas O. Binford, Ph.D. thesis, University of Wisconsin, 1965 (unpublished).

¹¹ Jared A. Anderson, Ph.D. thesis, Lawrence Radiation Laboratory Report No. UCRL-10838, 1963 (unpublished).

¹² Joseph A. Schwartz, Ph.D. thesis, Lawrence Radiation Laboratory Report No. UCRL-11360, 1964 (unpublished).

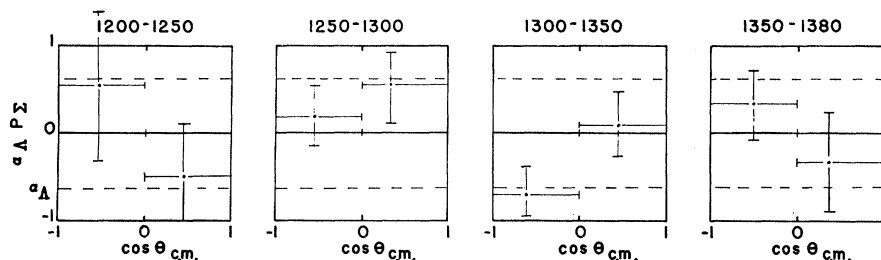


FIG. 6. Σ polarization in the form $\alpha_A P_\Sigma$ versus Σ^0 c.m. production angle for the π^- -beam momentum intervals shown.

curves represent cosine power-series fits. Although satisfactory fits with lower order were obtained in some cases, the third-order fits are shown because these were always satisfactory and never worse than the lower order fits, and because it is thereby possible to compare our data with Binford's at 1225 MeV/c and above, where third order was required. For purposes of comparison, our angular distributions have been normalized to 228 μb at 1275 MeV/c and to 225 μb at 1325 and 1365 MeV/c.¹³ Table I lists the cosine-series coefficients as functions of beam momentum (see Fig. 5).

C. Polarization

Figure 6 shows the Σ^0 polarization as a function of the c.m. production angle of the Σ^0 with the events divided into four momentum bins and two production-angle bins. We note that the Σ^0 polarization averaged over all events is very small. Statistically significant polariza-

tion is seen, however, in the backward hemisphere of Σ^0 production at 1325 MeV/c; the value obtained is $\alpha_A P_\Sigma = -0.71_{-0.25}^{+0.33}$. The errors are statistical only.

D. Discussion

The existence in the distribution at 1225 MeV/c of large $\cos^3\theta$ terms that are not present at 1170 MeV/c has been attributed by Binford¹⁰ to interference of $s_{1/2}$ and $f_{7/2}$ amplitudes. The $f_{7/2}$ amplitude is assumed to be large because of the 1920-MeV $N_{7/2}^*$ ($T = \frac{3}{2}$) resonance, which is centered at 1480 MeV/c in π^- momentum and has a half-width of 200 MeV/c. With a partial-wave analysis using s , p , and d waves only, Carayannopoulos *et al.* find a similar change in the odd-cosine series coefficients between 1111 and 1206 MeV/c in $\pi^+ + p \rightarrow \Sigma^+ + K^+$ (pure $T = \frac{3}{2}$).¹⁴ This seems to support Binford's interpretation. The angular distributions found in the present experiment also support Binford's interpretation, because the odd-cosine-series coefficients continue to dominate up to 1376 MeV/c. We note, however, that the Σ^0 polarization seems to change rapidly in the 1200–1400 MeV/c region. Figure 7 shows the forward-backward asymmetry (the difference between \bar{P}_Σ averaged over the forward hemisphere and \bar{P}_Σ averaged over the backward hemisphere). Although the data are not statistically compelling, this function appears to vary greatly with energy. Because the polarization is not likely to vary rapidly with energy if the angular distribution is dominated by a single interference term involving a broad resonance, the data suggest that the interaction may be more complicated than simple $s_{1/2}$ - $f_{7/2}$ interference.

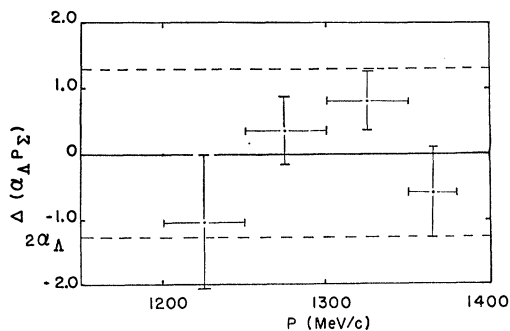


FIG. 7. $\alpha_A P_\Sigma$ for the forward Σ^0 production hemisphere minus $\alpha_A P_\Sigma$ for the backward hemisphere as a function of pion beam momentum.

¹³ We gratefully acknowledge receipt of these prepublication values from T. O. Binford.

¹⁴ N. L. Carayannopoulos, G. W. Tauffest, and R. B. Willman, Phys. Rev. **138**, B433 (1965).